Dynamic Flow Rate System for Ventricular Assist Devices

Rahul Gandhi
Jonathan LeMoel
Tian Xia

05/13/14

TABLE OF CONTENTS

BACKGROUND

Heart failure results in very high mortality and morbidity for those suffered. Now the gold-standard treatment for end-stage heart failure is still heart transplantation. However the number of donor hearts are very limited. As a result, implantable mechanical circulatory devices (MCDs) have come up as another option for improving survival in these patients. Among the MCDs, LVAD is widely used and performs well. For example, a 2009 study found 46 percent of HeartMate II (a product from Thoratec) patients were alive after two years without a stroke or repairs on the device, compared with 11 percent of those getting medical management [1][2].

There has been three generations of LVADs. Inherently, first-generation devices had larger tissue and blood contacting surfaces as well as multiple moving parts. The major disadvantages included comfort/ease of use for patients and long-term mechanical durability of the pump. Furthermore, high risk of infection, thrombus formation, and blood trauma were significant complications. The second generation uses valveless axial and continuous flow pump with a rotary motor as the only moving part in the system. Of importance were further enhancements of efficiency, durability, and patient outcomes [2]. The third generation LVAD employs the contact versus noncontact bearings. Centrifugal pumps could afford certain advantages that include lower rotational speeds, higher efficiency, and further enhanced anatomic design.

At present, most clinically implanted rotary blood pumps are operated at constant speed and adjusted by the manual-control approach such as the Jarvik 2000 [3]. At constant speed, changes in the remaining cardiac activity cause a minor adaptation

of pump flow to physiologic demand [4][5]. However, this increase remains below the natural response owing to the Frank-Starling mechanism.[6][7]. Therefore, to avoid over-pumping with subsequent collapse of the left ventricle and impairment of right heart function owing to septal shift [8] a speed-control system capable of adapting to the patient's physiologic requirements would provide additional clinical benefit [9].

In this project, an automatic speed control was developed and implemented by creating a feedback mechanism that would determine whether or not the user was being active. This would then adjust the RPM of the pump, allowing the patent to see an increase in blood flow when under physical stress.

MOTIVATION

Currently, artificial heart pumps do not have dynamic flow sensors pumping blood throughout the heart. A fixed flow rate, typically that between 5 and 6 liters/min is set for patients. This becomes problematic if the patient begins to undergo excessive physical exertion when walking up a hill or in case of emergency because the body is not able to adjust and provide extra oxygen throughout. Currently, the only device that allows any control at all is that of the Jarvik. This device allows the user to adjust a dial and change the flow rate.

During our trip to New York Presbyterian hospital, we learned that patients felt more alert and "smarter" after the implementation of the LVAD. This is thought to be due to an increase in the amount of blood and oxygen going to the brain and the remainder of the body. This shows the importance of a sufficient amount of blood flow. In instances where the body is undergoing physical exertion, an increase in blood flow is necessary to help energize the body. The normal heart rate for a human is between 5 to 6 liters/min. We expect current heart pump to be set to a value similar to this, however, the Heartmate II has the ability to pump up to 10 liters/min. This leaves a comfortable amount of room for the current heart pumps to increase depending on patient needs throughout the day.

While the typical heart pump patient is not expected to have too much physical activity outside of walking or climbing stairs, these activities still put the patient under stress and tires them out. If the heart pump came with a device that would monitor physical activity and adjust the blood flow rate automatically, the patient's quality of life would likely improve.

In order to accomplish this, ***we propose using accelerometers or a gyroscope to sense patient activity and calibrate the heart pump speed accordingly***. The device would be attached to the chest and is needed to differentiate between various conditions the patient may be undergoing. Since the pump would show a gradual change, the intensity of walking and climbing

steps also needs to be accounted for. The biggest factor that must be avoided is mixing up readings between physical activity and a bumpy car ride. The objective is to differentiate from the patient sitting, to walking, fast walking, and climbing stairs.

OVERALL LAYOUT

A 3D model [10] of the overall mechanical layout of the LVAD device is shown in figure 1.

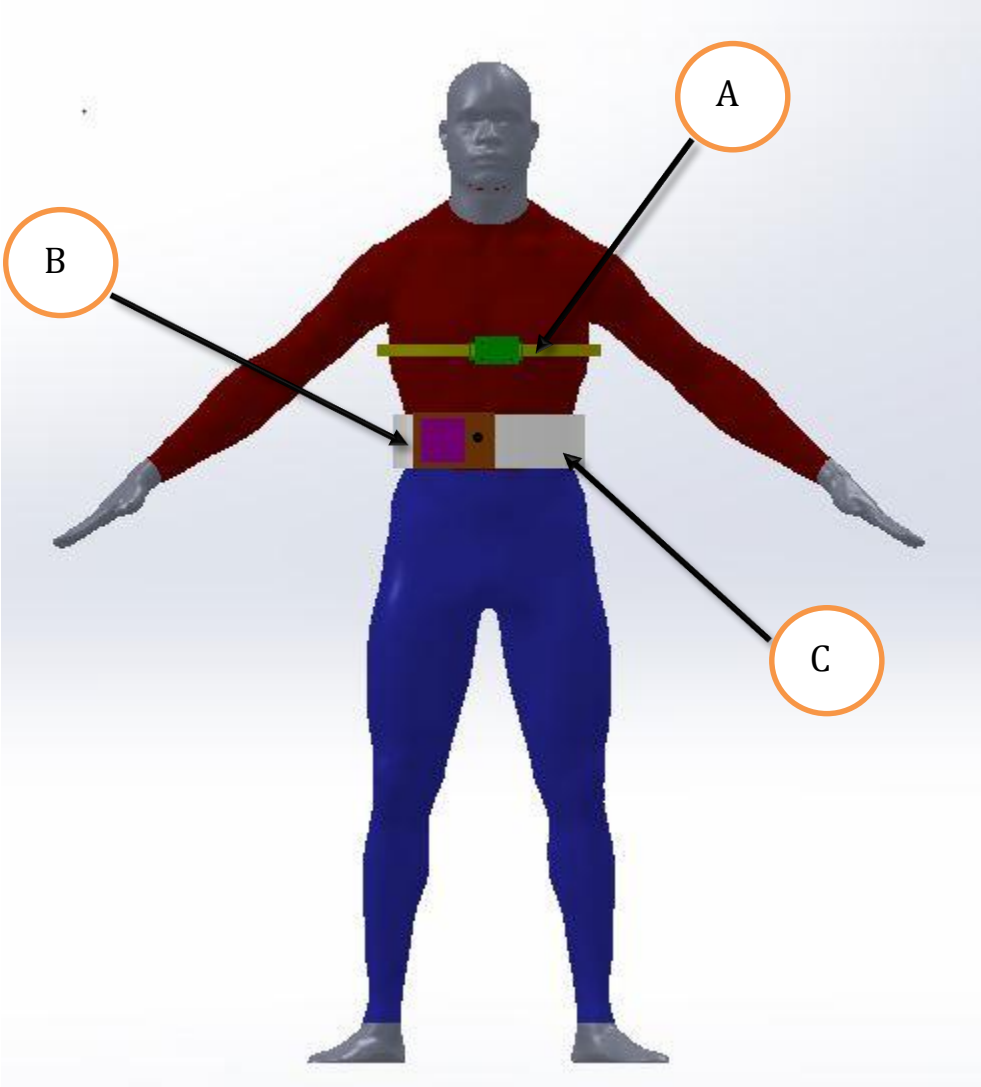

Figure 1 Mechanical layout of the LVAD device

The pump is inside the chest [11]. And in figure 1, label B is the system controller which contains the battery, (the magenta square) on the controller is the screen which would show the parameter of the LVAD. User could change the speed of the pump manually

by the black knob. The (label C grey band) is used for supporting the controller. In particular, the (label A green block) is the accelerometer supported by the yellow band. The accelerometer is able to measure the activity level of the person, sending this information back to the controller, which would change the pump speed based on that feedback data so that patient would get proper amount of blood driven by the pump automatically. No wire is shown in figure 1, for ultimately the communication among the controller modules, accelerometer and pump could be made through some wireless methods such as wifi and transcutaneous energy transmission system.

SENSOR SYSTEM DESIGN

The sensor system consists of electronic sensor, physical case and data link. The electronic sensor is an accelerometer used to measure the activity of the person. The physical case is used to protect the sensor and attach the sensor to the human body. The data link is used to connect the sensor to the controller.

In order to collect some movement data of human by accelerometer so that further analysis is possible, firstly there should be a case to hold and protect the accelerometer during the test, the case is also useful for attaching the accelerometer to the human body.

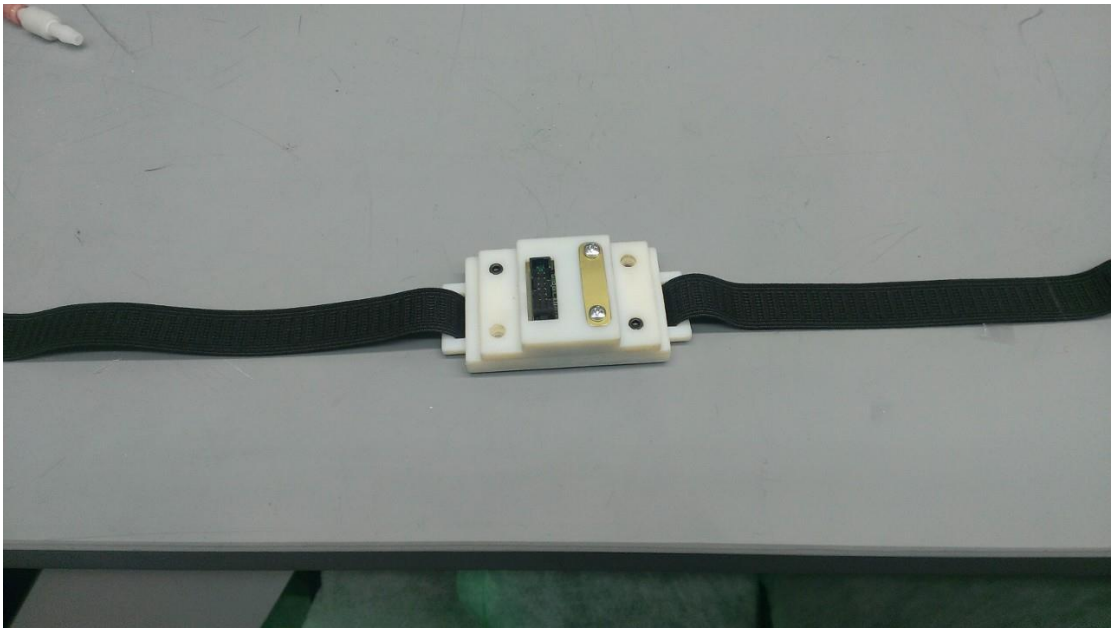

Figure 2 Fabricated sensor system using KX0230 accelerometer

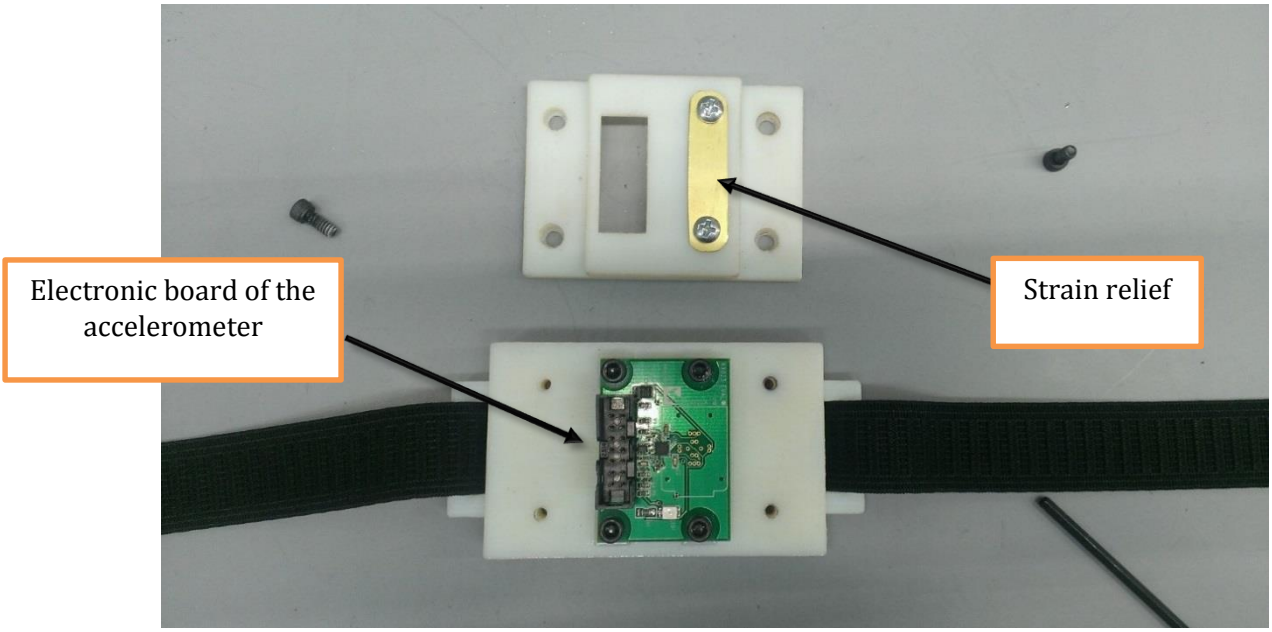

Figure 3 Inside structure of the case (1)

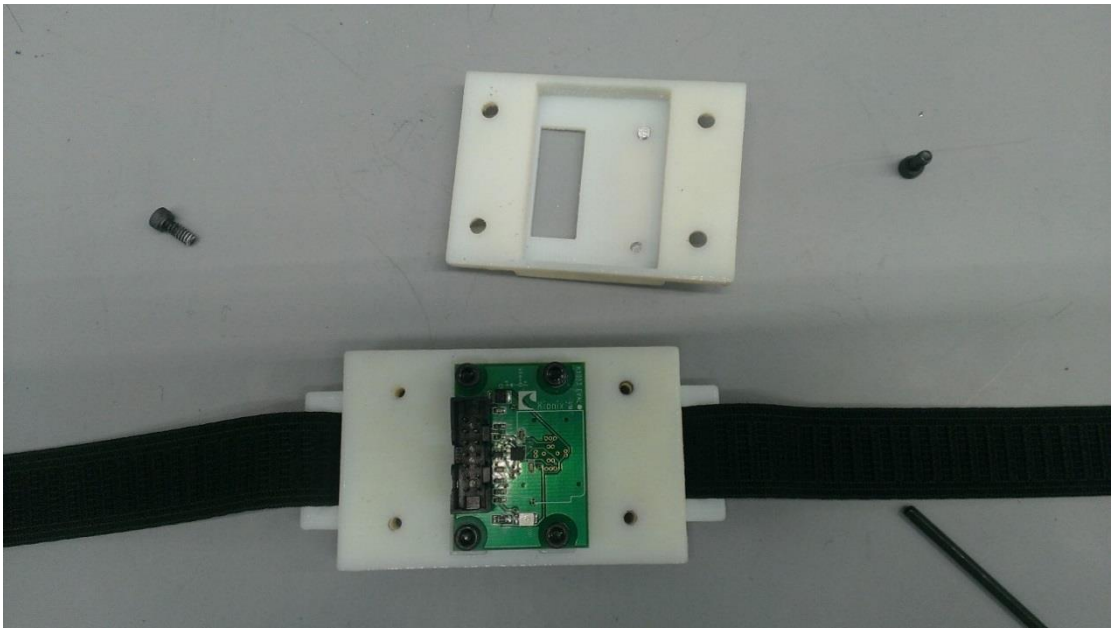

Figure 4 Inside structure of the case (2)

Figure 2 above is the case with the accelerometer inside it. Firstly, many factors were taken into consideration in the design process. Since the accelerometer is small, the whole case should also be small for we don't want to waste material and bigger, heavier case would make patient wearing it feel uncomfortable. Thus a challenge was packaging all the necessary features in a limited 50 grams, 40 cubic centimeters case. Band attachment used two slots on either end of the case. In designing the lid, there is a hole on the lid for the ribbon connector to pass through. And the height of the lid has to be lower than that of the ribbon connector on the accelerometer to make sure there is enough room to connect to the ribbon. The gold bar with screws on each end is a strain-relief. In addition all the corners are softened to make it a wearable device.

After designing, the model needs to be fabricated. Primary fabrication work was done by 3D printing from Incodema3D, followed by drilling and tapping all the ten thread

holes ourselves, since the diameter of the thread hole is only about 3.5mm, which is hard to form by 3D printing. During the design stage, there are already 10 holes with diameter of 1mm to mark the location of each hole. Then the drilling machine was used to drill the holes. After that, the thread holes were tapped manually, as shown in figure 5. Besides, an elastic band is passed through the two handles of case, the length of which is adjustable so that it is able to fit the body of different people.

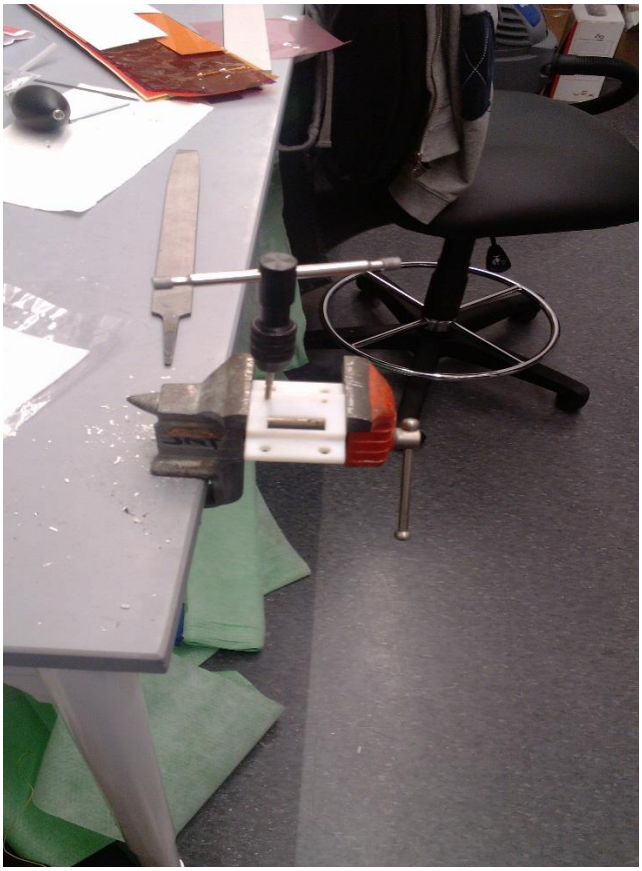

Figure 5 Tapping the thread hole

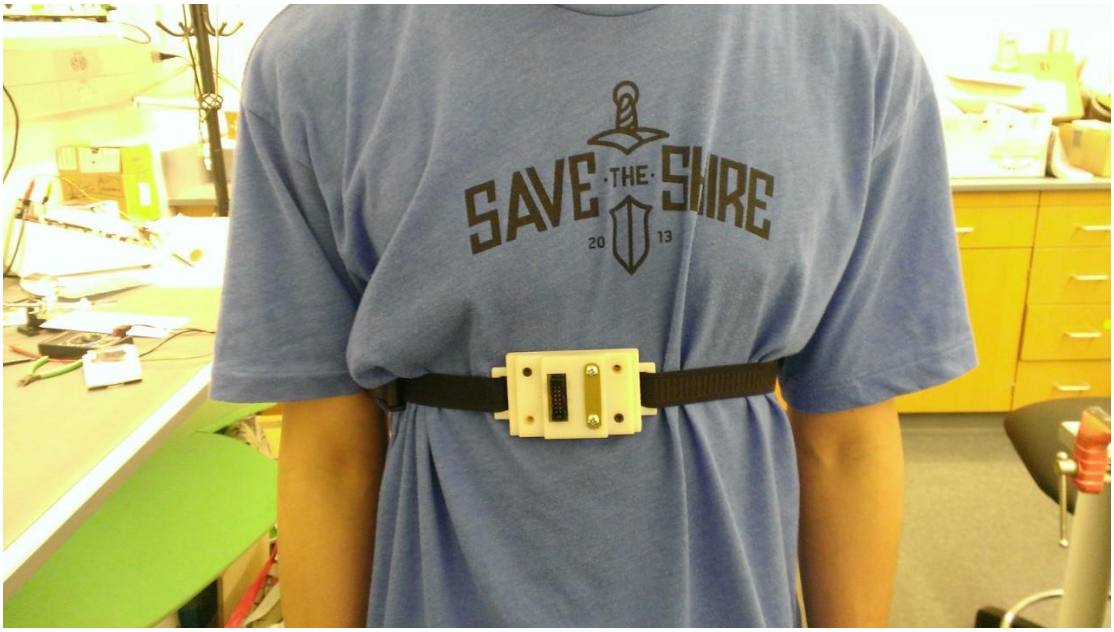

Figure 6 One person wearing the case with accelerometer

Having done all of the work above, the device was assembled from the parts and the accelerometer. The case with the accelerometer inside it was worn during tests and worked as expected with minimal movement, as shown in figure 6.

In order to create a device that would measure physical movement, accelerometers were obtained from Kionix and used to gather data [Figure 7]. Due to time constraints, preliminary testing was done by placing the accelerometer in a plastic static free bag [Figure 8]. This was then connected to the laptop and real time data acquisition was done using Kionix proprietary software [Figure 9].

Figure 7

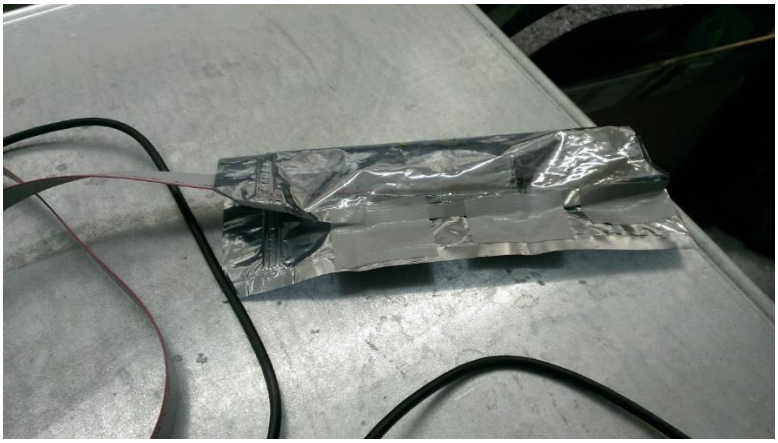

Figure 8

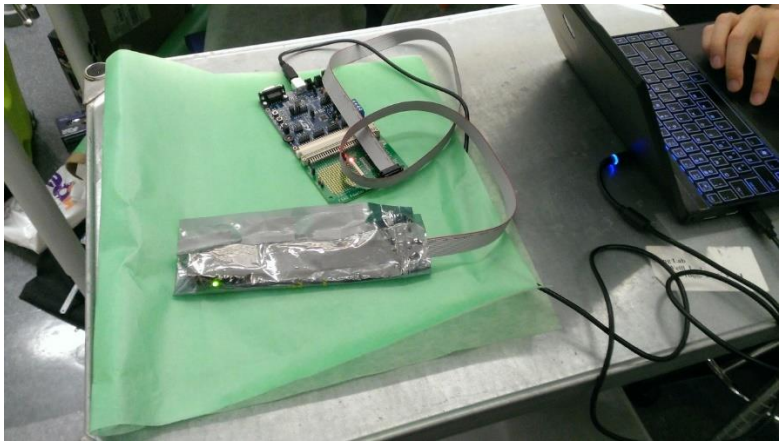

Figure 9

After attaching the device to the right side of the chest, four separate trials were run. The same trials were repeated again but with the device attached to the left side of the chest. This was done to see a correlation, if any, between the location of the device and the foot pushing off. In order to ensure different walking styles, a second subject was also used to support preliminary results.

Figure 10

Initially, the user was recorded walking along a hallway at slow/normal speed. The second trial was with the user walking as fast as they can while keeping a steady pace to show a consistent

trend in the data. The next run was up and down a long stairway. During this run, the user yelled "step" every time a step was taken using the foot on the same side as the accelerometer. This was done to help correlate the observed trends with what the user was actually doing. The final run was sitting in the passenger seat of a car as it drove around the Cornell University campus at 20 to 30 mph. For this run, the car stopped and went at the appropriate stop signs and took both left and right turns to properly emulate a normal driving scenario.

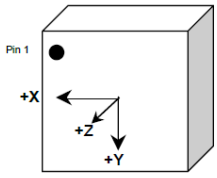

Static X/Y/Z Output Response versus Orientation to Earth's surface (1g):

GSEL1=0, GSEL0=0 (± 2g)

Position	1		2		3		4		5		6	
Diagram									Top Bottom		Bottom Top	
Resolution (bits)	16	8	16	8	16	8	16	8	16	8	16	8
X (counts)	0	0	-16384	-64	0	0	16384	64	0	0	0	0
Y (counts)	-16384	-64	0	0	16384	64	0	0	0	0	0	0
Z (counts)	0	0	0	0	0	0	0	0	16384	64	-16384	-64
X-Polarity	**0**		**-**		**0**		**+**		**0**		**0**	
Y-Polarity	**-**		**0**		**+**		**0**		**0**		**0**	
Z-Polarity	**0**		**0**		**0**		**0**		**+**		**-**	

In each of the data sets collected, the raw data is output from the accelerometer in counts. These counts can then be converted into gravitational units (g). The output counts range from 32768 to -32768 where 32768 corresponds to 2g and -32768 corresponds to -2g. This is because the accelerometer is set up in the 2g range. Due to the nature of the tests, it is unnecessary to set the device up into the max 8g range.

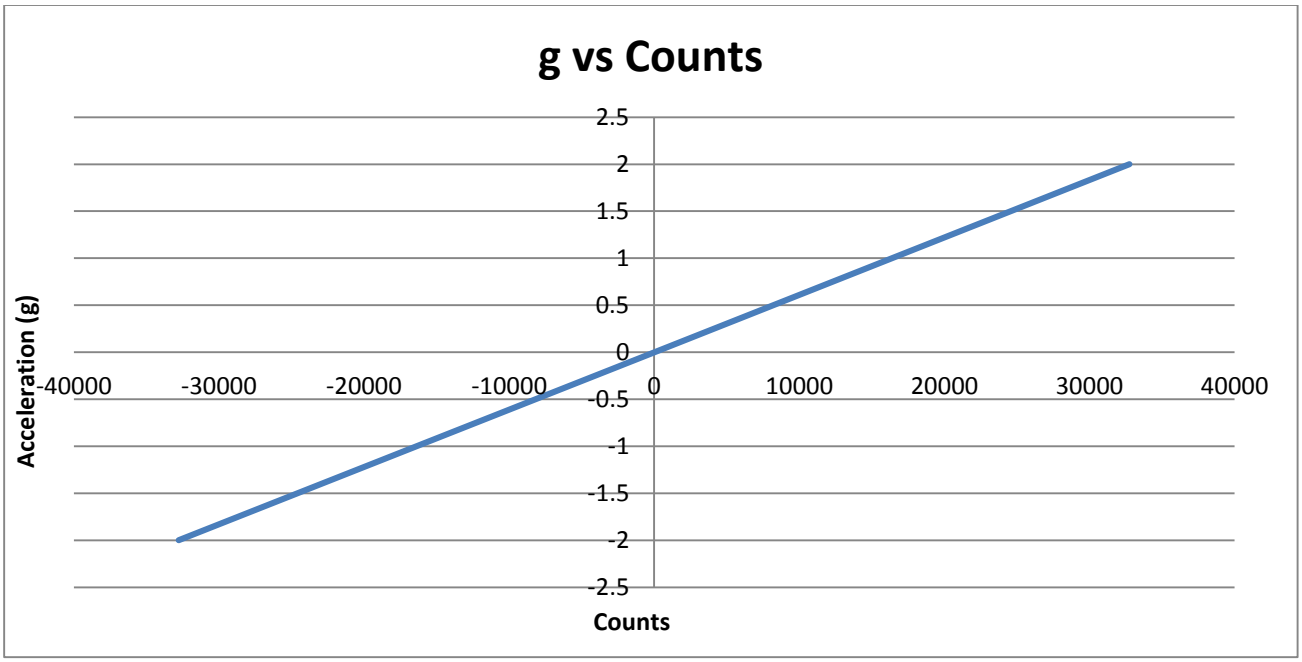
g vs Counts
Acceleration (g)
2.5
2
1.5
1
0.5
0
-0.5
-1
-1.5
-2
-2.5
-40000
-30000
-20000
-10000
0
10000
20000
30000
40000
Counts

Baseline

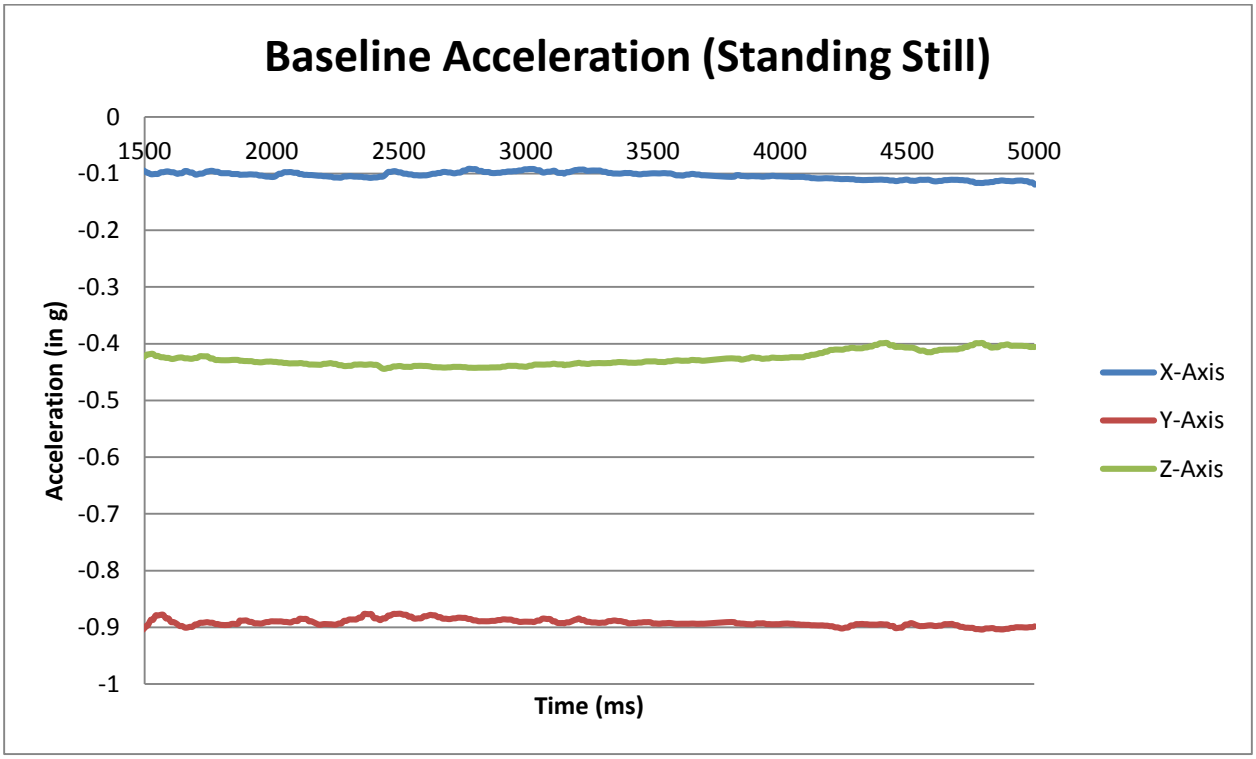
Baseline Acceleration (Standing Still)
Acceleration (in g)
0
-0.1
-0.2
-0.3
-0.4
-0.5
-0.6
-0.7
-0.8
-0.9
-1
1500
2000
2500
3000
3500
4000
4500
5000
Time (ms)
X-Axis
Y-Axis
Z-Axis

Walk

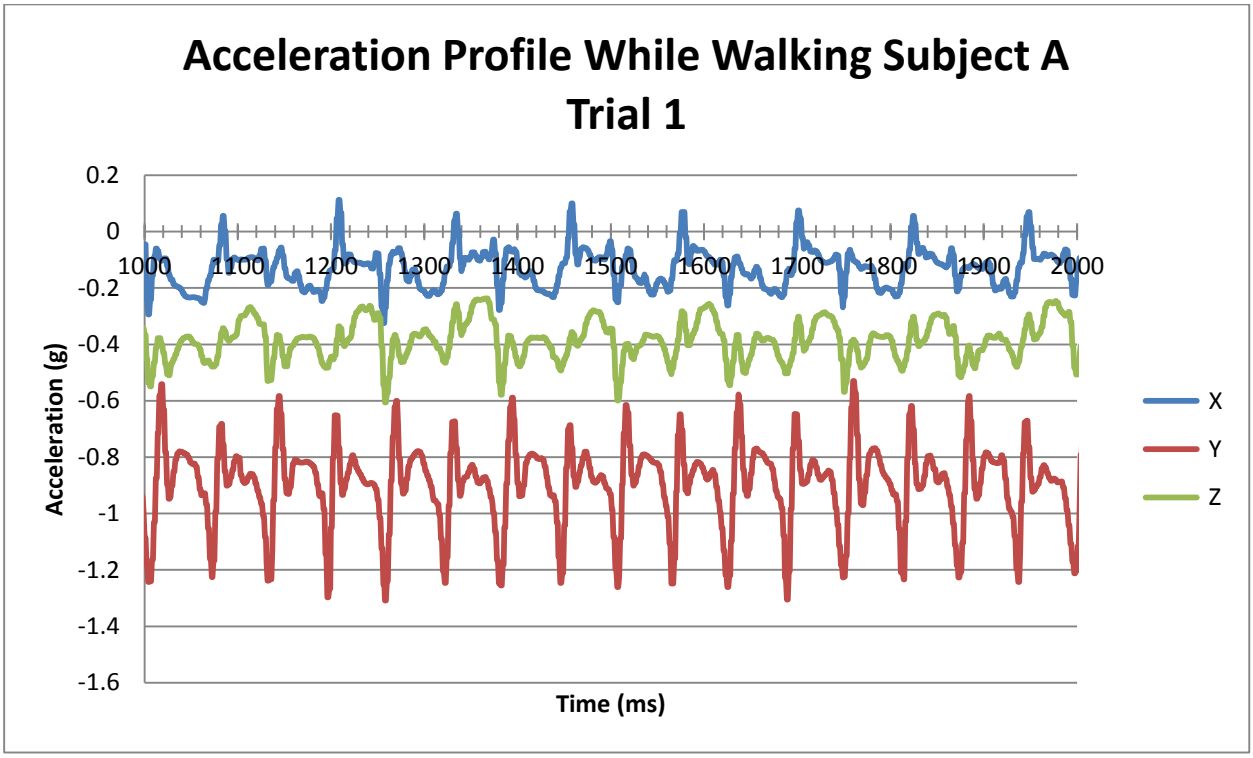
Acceleration Profile While Walking Subject A
Trial 1
0.2
0
-0.2
-0.4
-0.6
-0.8
-1
-1.2
-1.4
-1.6
1000
1100
1200
1300
1400
1500
1600
1700
1800
1900
2000
Acceleration (g)
Time (ms)
X
Y
Z

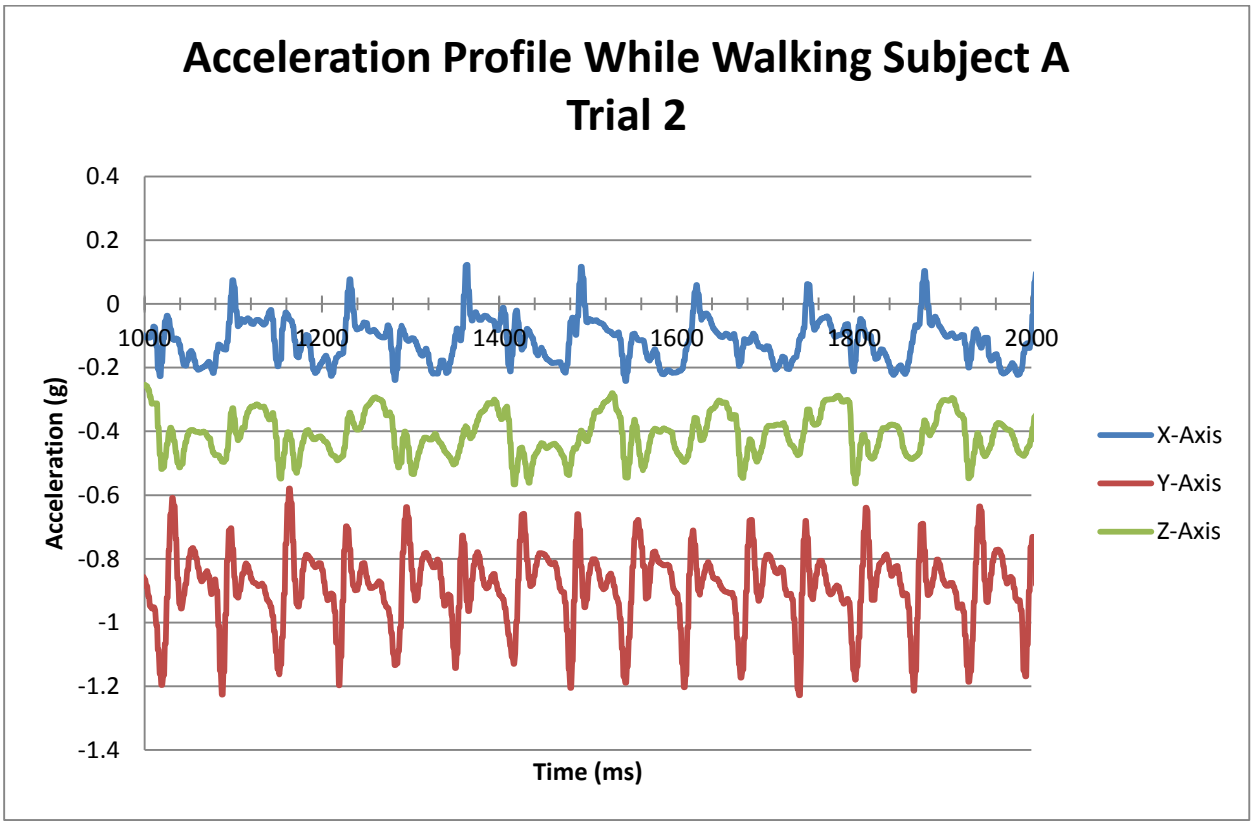
Acceleration Profile While Walking Subject A
Trial 2
0.4
0.2
0
-0.2
-0.4
-0.6
-0.8
-1
-1.2
-1.4
1000
1200
1400
1600
1800
2000
Acceleration (g)
Time (ms)
X-Axis
Y-Axis
Z-Axis

Fast Walk

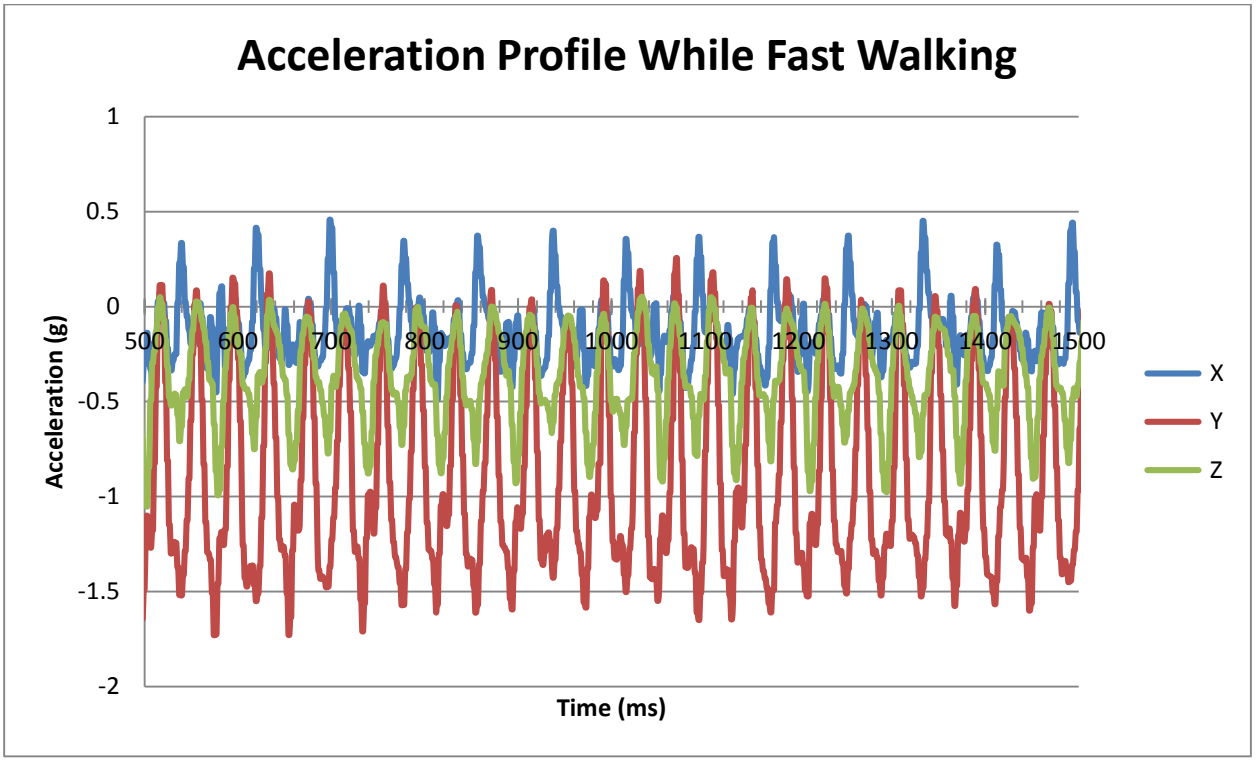
Acceleration Profile While Fast Walking
1
0.5
0
-0.5
-1
-1.5
-2
Acceleration (g)
500
600
700
800
900
1000
1100
1200
1300
1400
1500
Time (ms)
X
Y
Z

Stairs

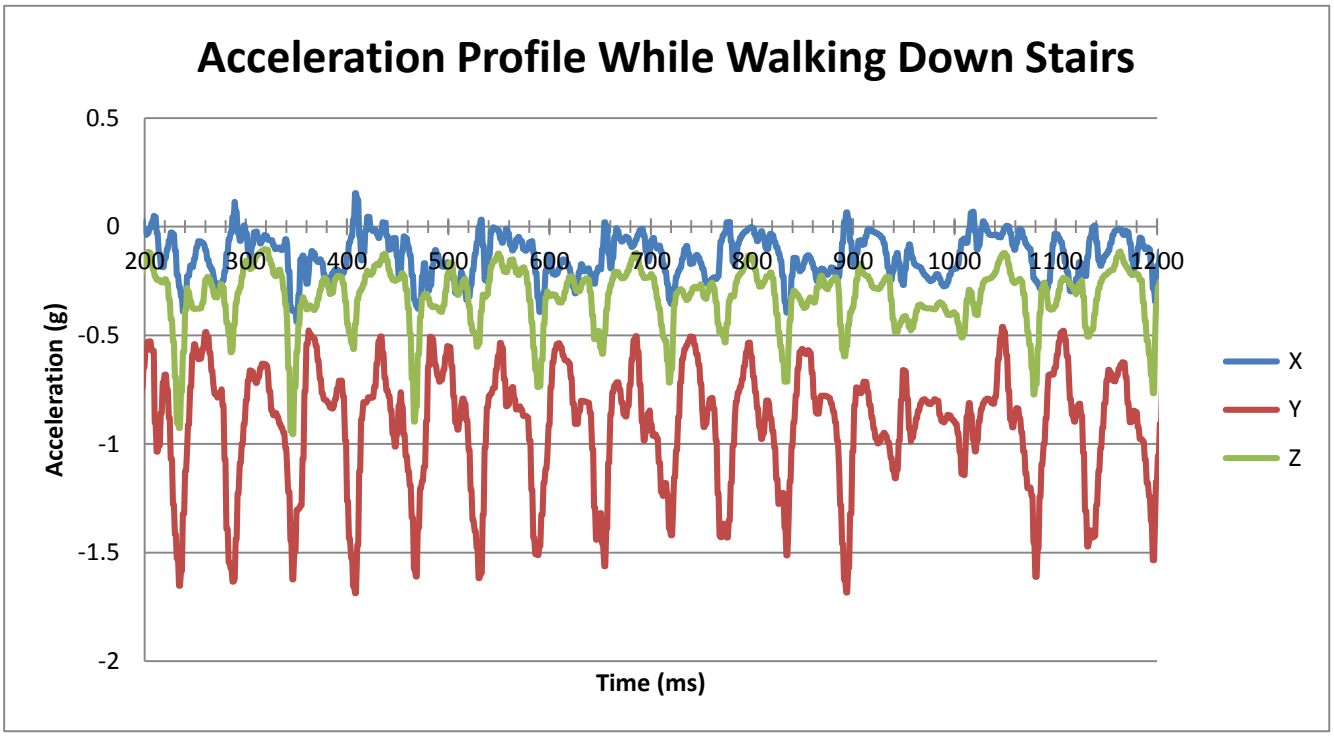
Acceleration Profile While Walking Down Stairs
0.5
0
-0.5
-1
-1.5
-2
200
300
400
500
600
700
800
900
1000
1100
1200
Acceleration (g)
Time (ms)
X
Y
Z

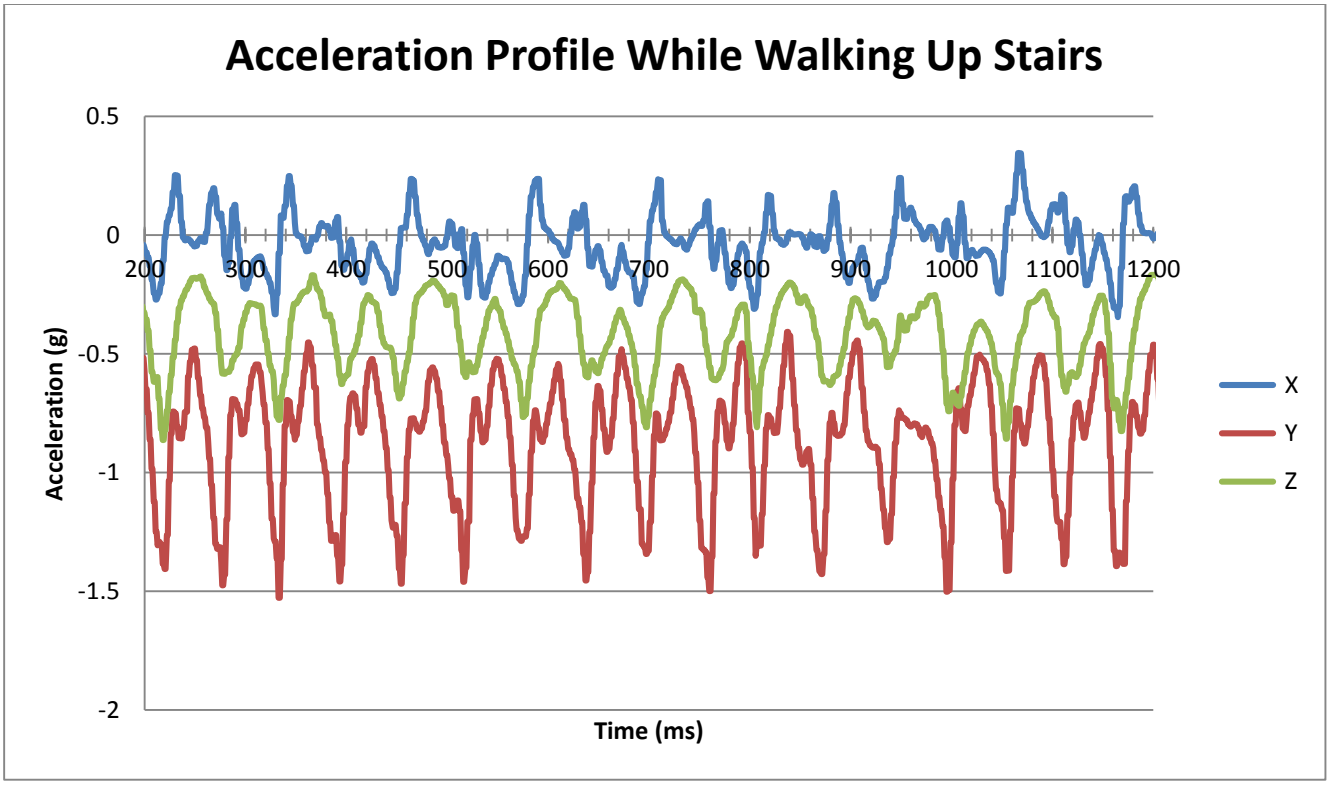
Acceleration Profile While Walking Up Stairs
0.5
0
-0.5
-1
-1.5
-2
200
300
400
500
600
700
800
900
1000
1100
1200
Acceleration (g)
Time (ms)
X
Y
Z

Car

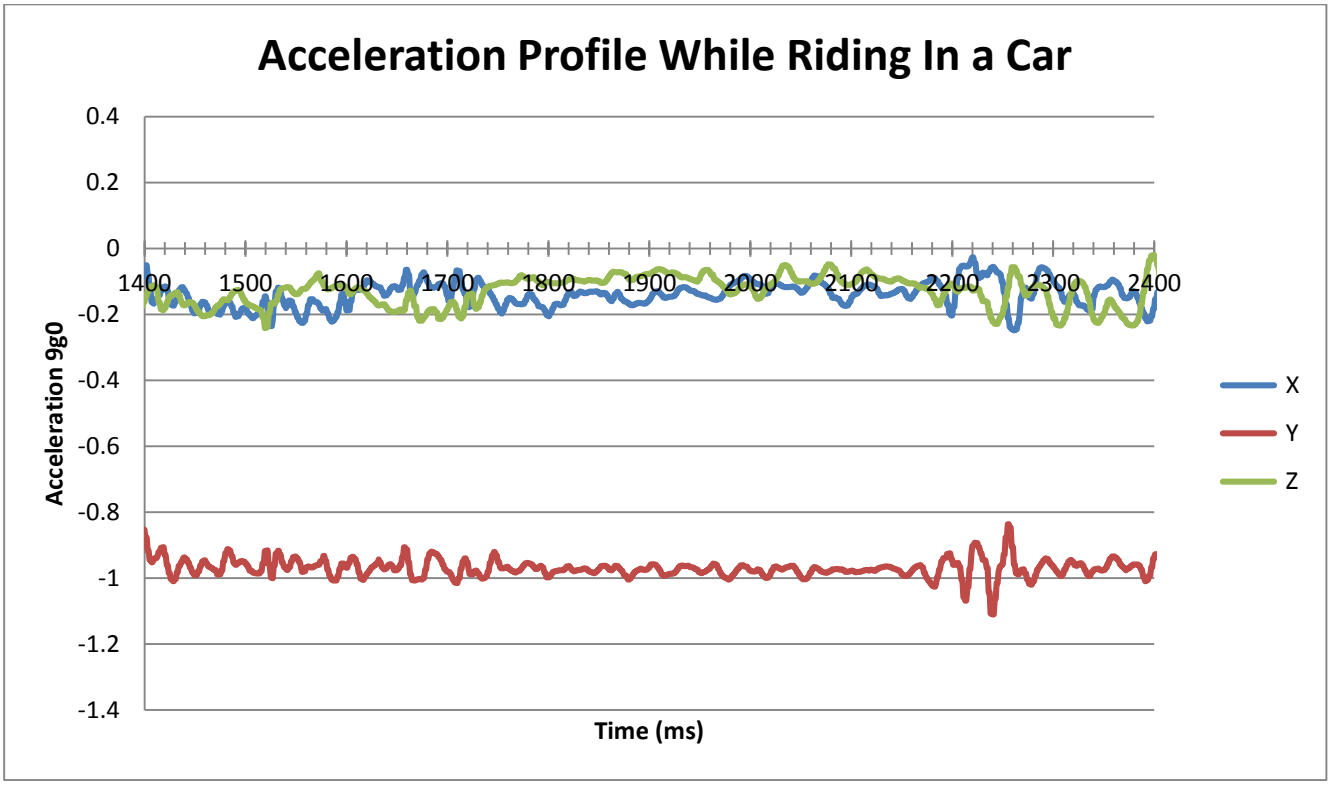
Acceleration Profile While Riding In a Car
0.4
0.2
0
-0.2
-0.4
-0.6
-0.8
-1
-1.2
-1.4
1400
1500
1600
1700
1800
1900
2000
2100
2200
2300
2400
Acceleration 9g0
Time (ms)
X
Y
Z

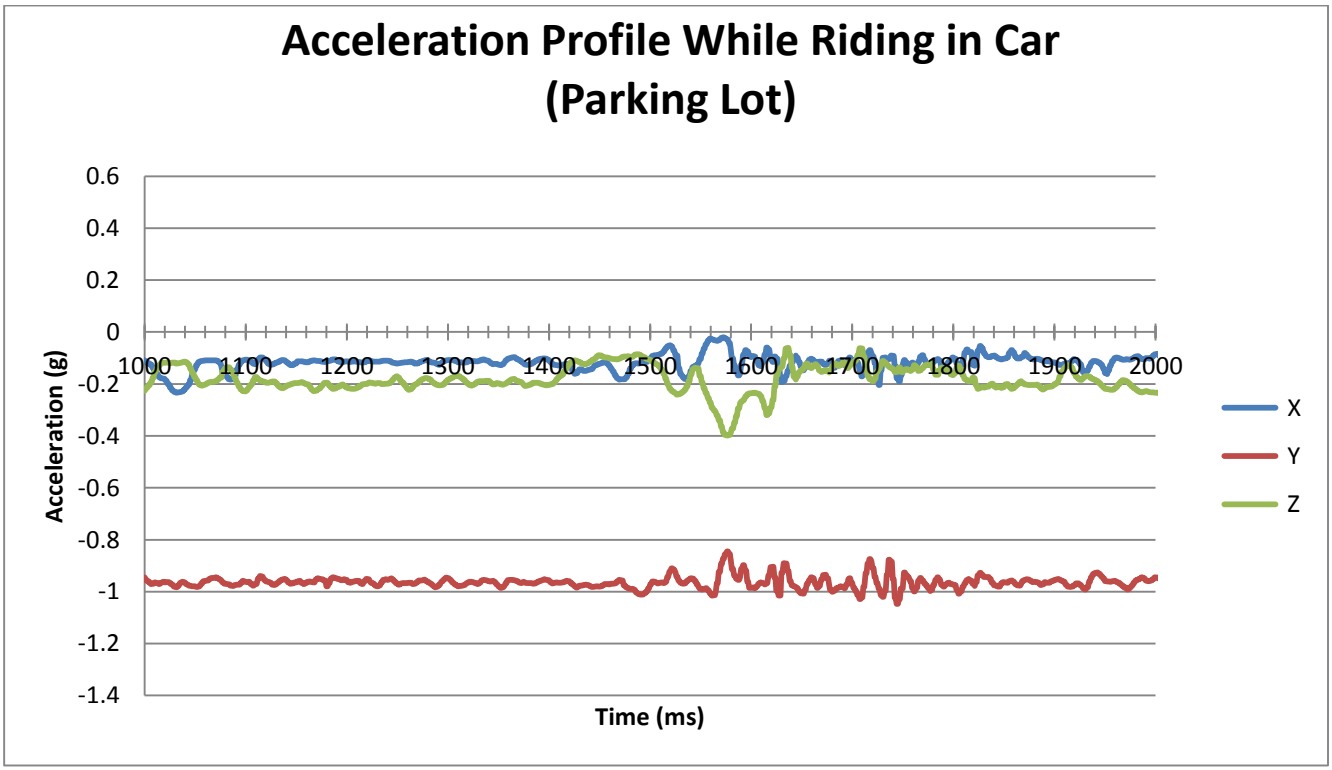
Acceleration Profile While Riding in Car
(Parking Lot)
0.6
0.4
0.2
0
-0.2
-0.4
-0.6
-0.8
-1
-1.2
-1.4
1000
1100
1200
1300
1400
1500
1600
1700
1800
1900
2000
Acceleration (g)
Time (ms)
X
Y
Z

Subject 2

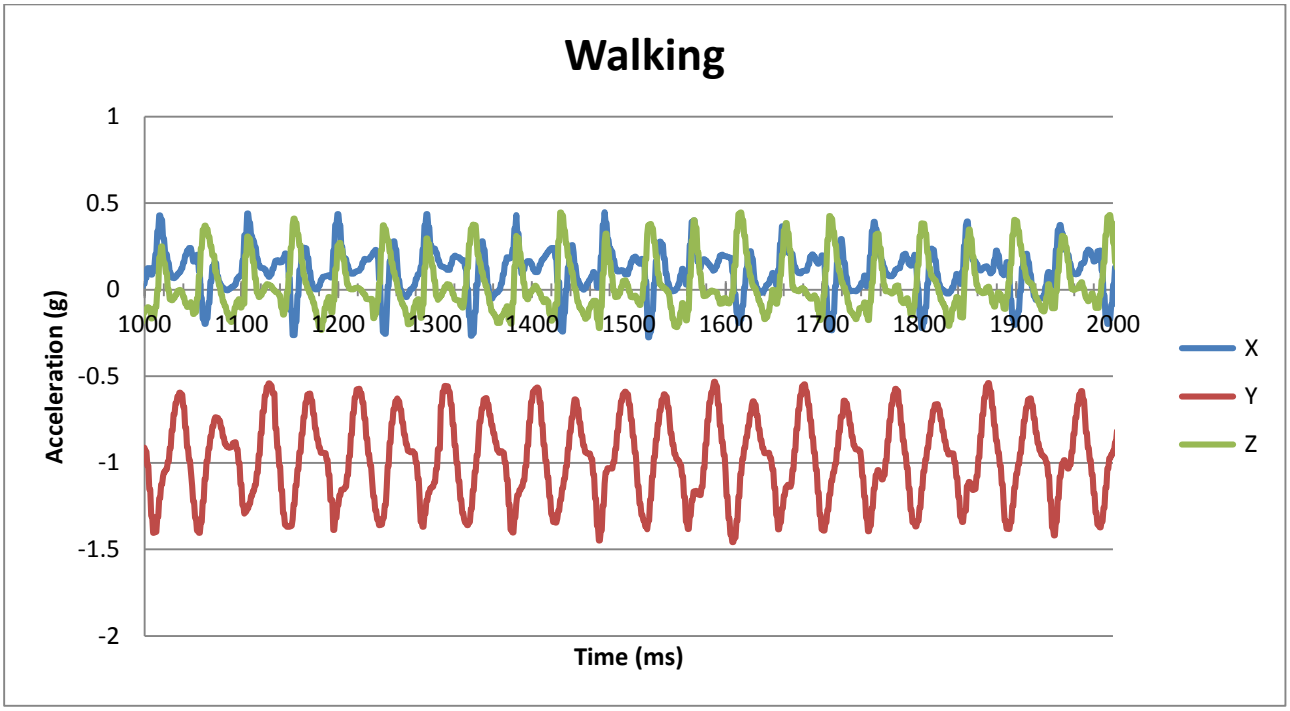
Walking
1
0.5
0
-0.5
-1
-1.5
-2
1000
1100
1200
1300
1400
1500
1600
1700
1800
1900
2000
Acceleration (g)
Time (ms)
X
Y
Z


Fast Walking
1
0.5
0
-0.5
-1
-1.5
-2
1000
1100
1200
1300
1400
1500
1600
1700
1800
1900
2000
Acceleration (g)
Time (ms)
X
Y
Z

The acceleration profiles generated in the tests show that distinct patterns do indeed exist in each of the various activities. In the first set of graphs the conversion from counts to gs is shown for a baseline subject. This test was carried out to determine the resting positions of the axes as well as to gauge the noise of the device. Circled above, the ambient acceleration is minimal but there are some large deviations in overall gs as seen in the Z axis. This is most likely due to swaying of the subject while standing.

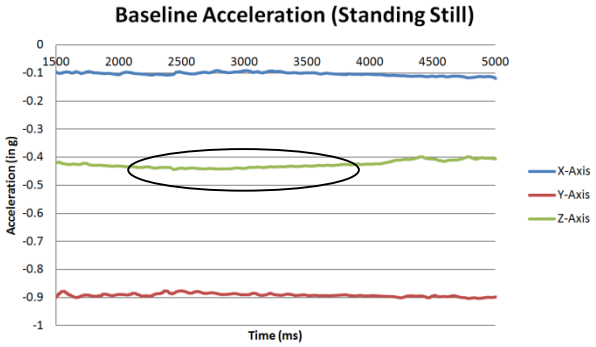

In the acceleration profile for walking, it is clear that there is a distinct cadence during the activity. The two graphs show that even over time and among numerous engagements in this activity, the profile remains distinct for that particular individual.

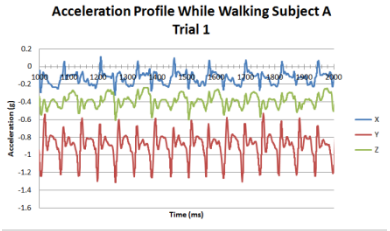

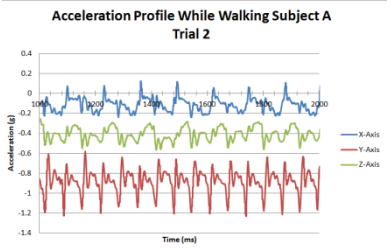

In the fast walking profile the pattern is very similar but there are a few key differences. As one might expect, the amplitude of each axis is larger meaning the motion in each direction is stronger. Second, the frequency of the pattern is higher. These are both simple parameters to check for in the algorithm, meaning distinguishing movement from other activities using these parameters may be simple.

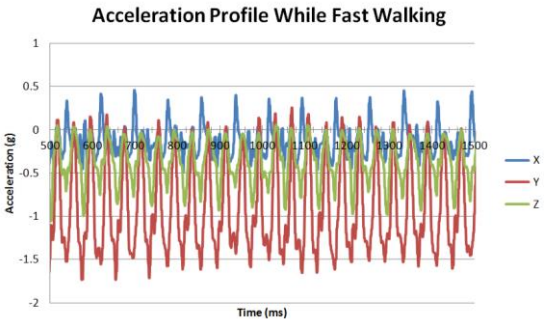

In the next set of graphs a simple straight staircase was walked, up and down. In this case, the goal was to observe any distinctions between the profiles of walking up and down stairs to that of walking across flat ground. The main difference here is still that of amplitude of impact, especially in the downward direction as signified by the Y-axis in this test configuration.

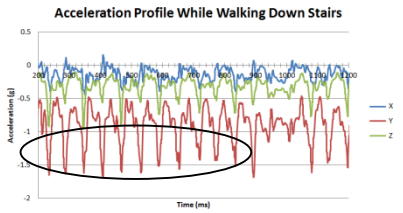

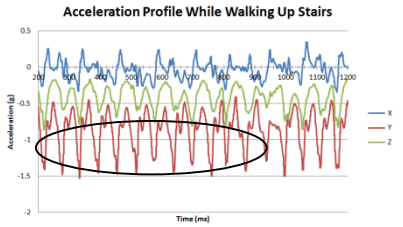

One of the most important aspects of the tests was to confirm that the movement exhibited by the body while riding in a moving vehicle could be distinguished from other activities such as walking. As seen in both car ride profiles, they differ greatly from the other activity profiles. In the car, amplitude changes in the downward direction are minimal, with spikes mainly due to road roughness. Even with impurities in the road, the changes are very small when compared to those amplitude changes while walking. An interesting phenomena exhibited by the car ride profile is that the X and Z axes seems to follow a counter acting pattern, as the X-axis increases the Z-axis decreases. This could be due to the nature of the body's inertia, causing such rotations as the car turns.

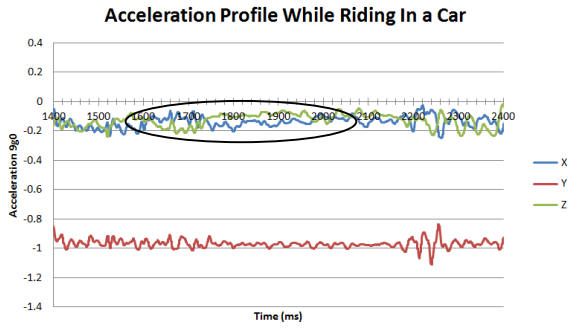

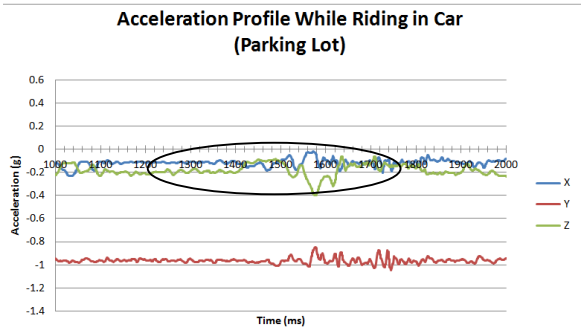

Finally, similarities in differences can be seen between multiple subjects suggesting that the same changes from activity to activity between each person is constant. This will enable for detection of a particular activity even though the exact pattern of the profile varies.

Subject B

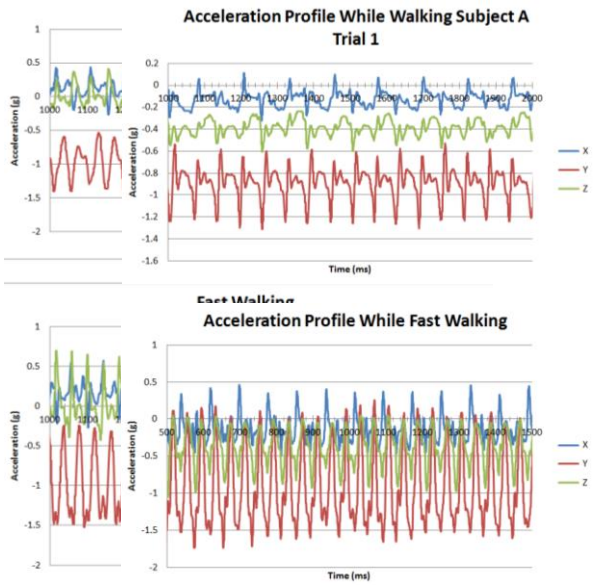

Subject A

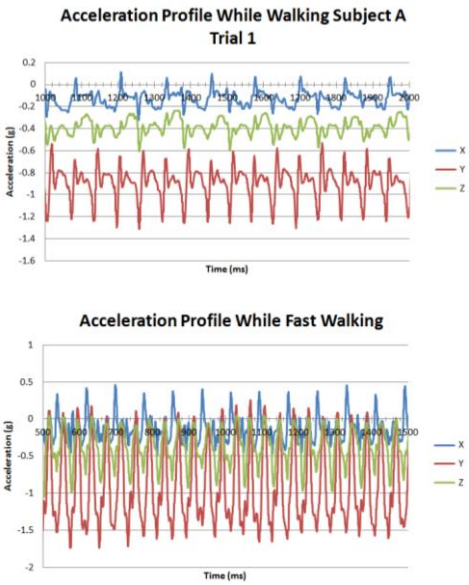

FUTURE WORK

The implications of the initial data suggest there are many more questions to answer. First the placement of the accelerometer on the body must be optimized. The tests carried out were all done with the device mounted on the subject's right chest. Similar tests should be conducted with the accelerometer on the left side as well as in the middle of the subject. In addition, vertical placement must also be considered.

These tests were also conducted with the device directly mounted to the subject's body. In the final device, it is likely that the accelerometer will be integrated into another unit due to space constraints. This will mean that the profiles will change based on the inertia of the device. These inertial effects must be accounted for in future tests and the effects of the internal mounting must also be made clear.

REFERENCES

1 Daniel Lee Crandall. Pre-clinical in vivo and in vitro assessment of hemostatic effects of continuous-flow ventricular assist devices. Ph.D. Thesis. Illinois Institute of Technology, July 2011.

2 Rodriguez LE, Suarez EE, Loebe M, Bruckner BA.Ventricular assist devices (VAD) therapy: new technology, new hope? *Methodist Debakey Cardiovasc* J. 2013 Jan-Mar;9(1):32-7.

3 JARVIK HEART, Inc, http://www.jarvikheart.com/basic.asp?id=21

4 Wieselthaler GM, Schima H, Hiesmayr M, et al. First clinical experience with the DeBakey VAD continuous axial-flow pump for bridge to transplantation. Circulation (US) 2000;101:356–9.

5 Akimoto T, Yamazaki K, Litwak P, et al. Rotary blood pump flow spontaneously increases during exercise under constant pump speed: results of a chronic study. Artif Organs 1999;23:797–801.

6. Farrar DJ, Buck KE, Coulter JH, Kupa EJ. Portable pneumatic biventricular driver for the Thoratec ventricular assist device. ASAIO J 1997;43:M631–4.

7. Miller PJ, Billich TJ, LaForge DH, et al. Initial clinical experience with a wearable controller for the Novacor left ventricular assist system. ASAIO J 1994;40:M465 70.

8. Vollkron M, Schima H, Huber L, Benkowski R, Morello G, Wieselthaler G. Development of a suction detection system for axial blood pumps. Artif Organs 2004;28:709–16.

9. Schima H1, Vollkron M, Jantsch U, et al. First Clinical Experience with an Automatic Control System for Rotary Blood Pumps During Ergometry and Right-Heart Catheterization. J Heart Lung Transplant. 2006 Feb;25(2):167-73.

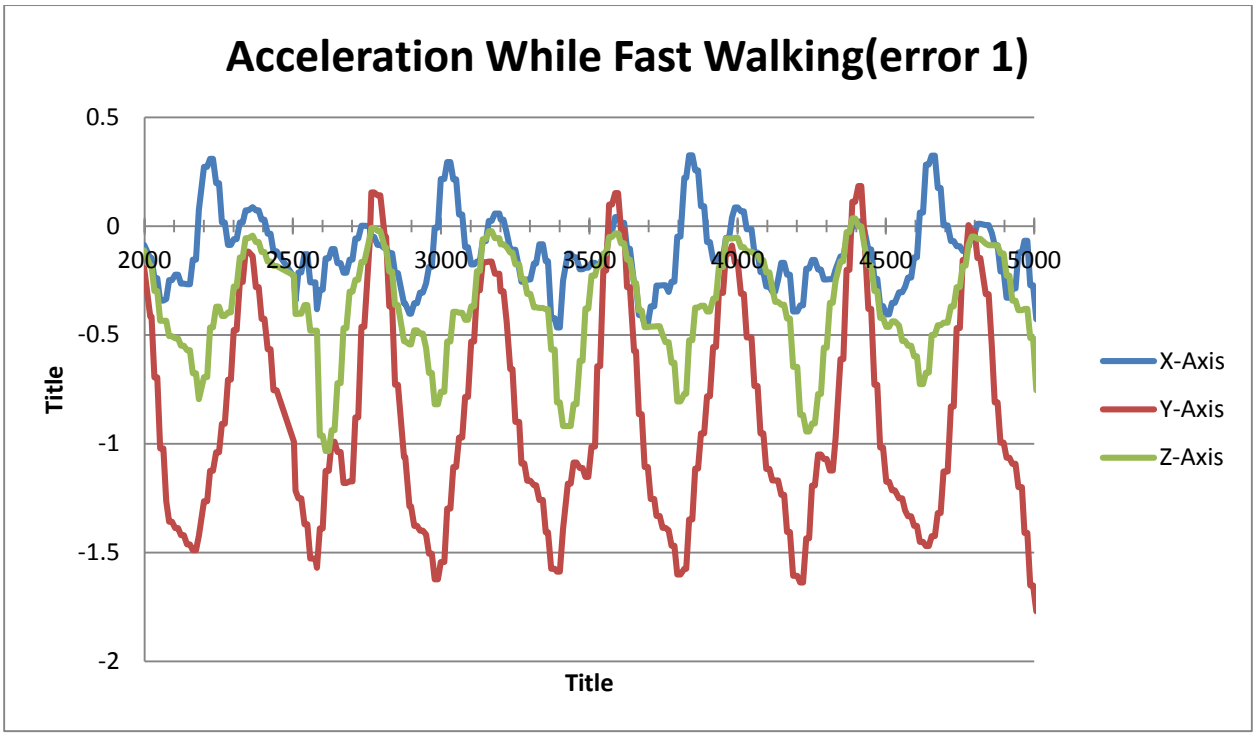
Acceleration While Fast Walking(error 1)
0.5
0
-0.5
-1
-1.5
-2
2000
2500
3000
3500
4000
4500
5000
Title
Title
X-Axis
Y-Axis
Z-Axis

Case Dimensions

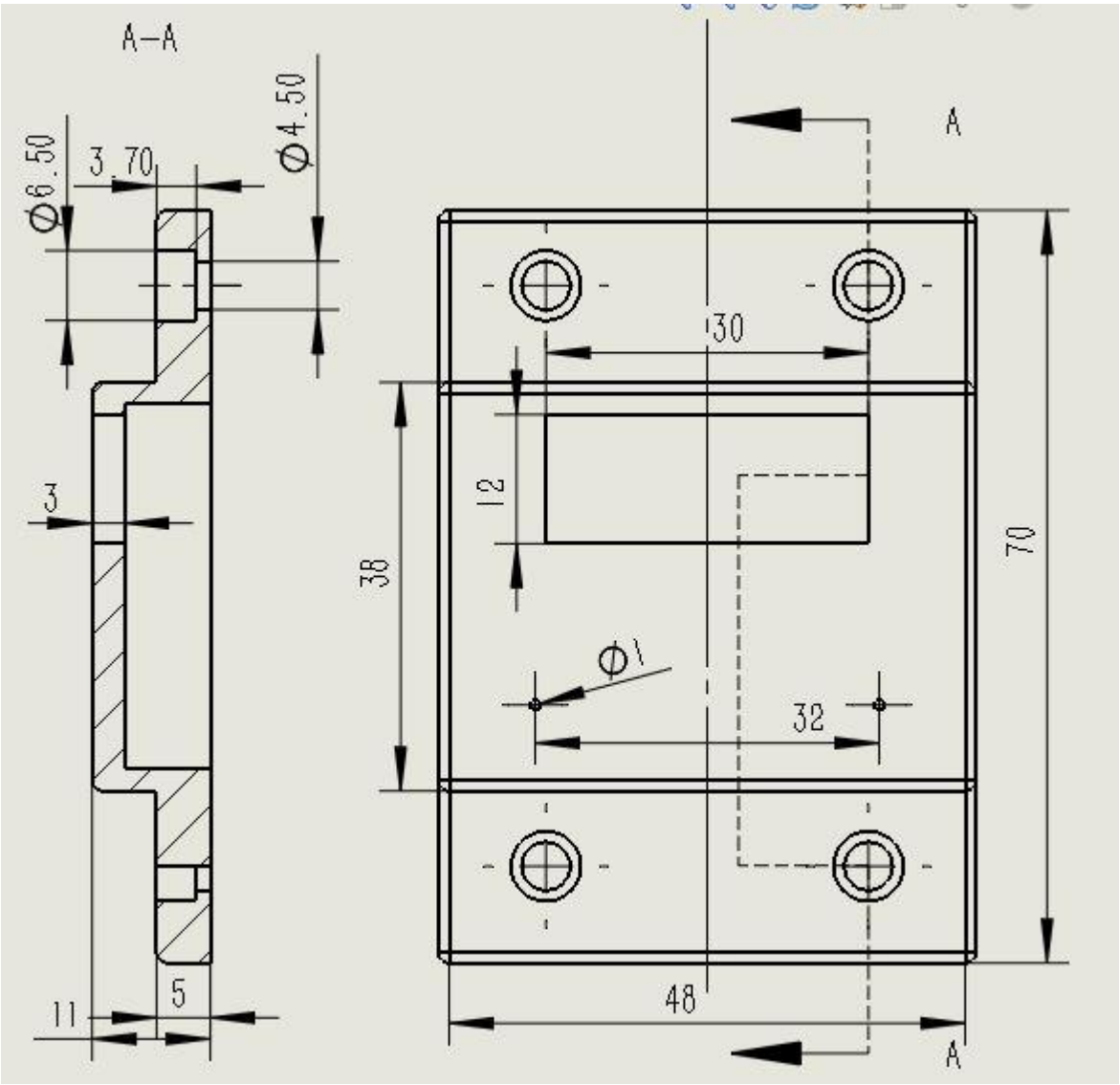

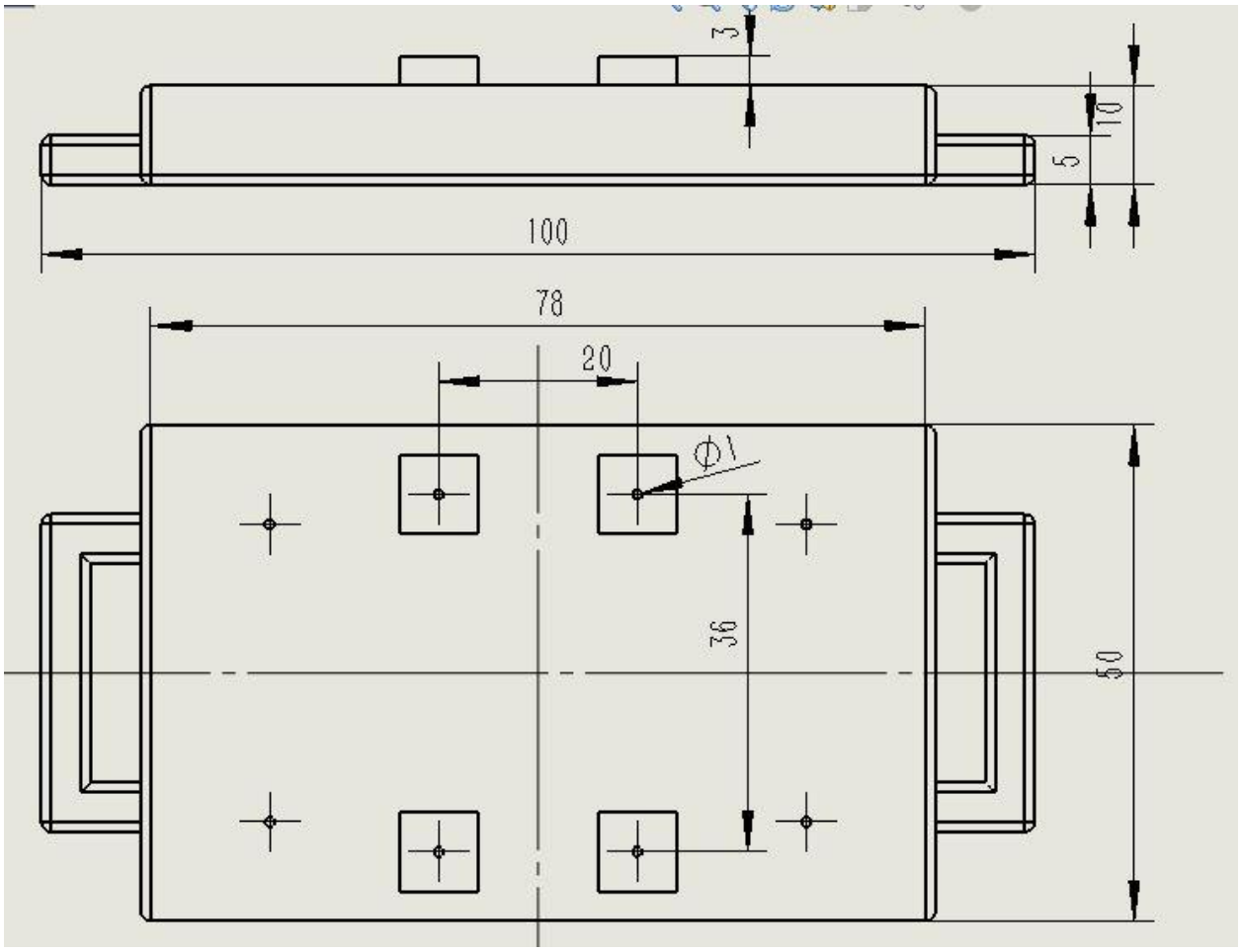
3
10
5
100
78
20
ϕ1
36
50